

STOCHASTIC DRILL-STRING DYNAMICS VIA COSSERAT ROD MODELS

Héctor E. Goicoechea^{a,b}, Fernando S. Buezas^{a,c}, Marta B. Rosales^{a,b} and Rubens Sampaio^d

^a*IFISUR, Universidad Nacional del Sur, CONICET, Departamento de Física - UNS, Av. L. N. Alem 1253, B8000CPB - Bahía Blanca, Argentina*

^b*Departamento de Ingeniería, Universidad Nacional del Sur, Av. Alem 1253, (8000) Bahía Blanca, Argentina*

^c*Departamento de Física, Universidad Nacional del Sur, Av. Alem 1253, (8000) Bahía Blanca, Argentina*

^d*Dept. of Mechanical Engineering, PUC-Rio, Rua Marquês de São Vicente 225, 22453-900 Rio de Janeiro, Brasil*

Keywords: drill-string, stochastic modelling, cosserat rod

Abstract. The study of drill-string dynamics is a complex matter. With lengths surpassing 1000 m, due to their slenderness, geometrical aspects of oil-wells and contact forces, drill-strings usually exhibit a highly non-linear response. Operative conditions are very sensitive to changes in working parameters, namely rotary speed and hook load, among others. Moreover, many unwanted phenomena may occur when conditions for stable operation are not met, such as stick-slip oscillations. On top of that, there are several intrinsic uncertainties, e.g. modelling of soil, which may lead to unwanted operation regimes that negatively affect performance, i.e. degraded rate-of-penetration (ROP). In this work, a stochastic approach to drill-string dynamics is presented via a Cosserat rod model. The model is implemented in a finite element environment. Nonlinearities of the drill-string problem occur due to geometrical factors such as finite displacements and rotations, as well as to contact and friction at the borehole wall and bit. In particular, a friction model presented by (R. Tucker and C. Wang, *Meccanica*, 38(1):143-159(2003)) is used. The drill is set in motion via a PI-Controller driving the motor at the top drive. First, the deterministic model is implemented using the weak formulation mathematical interface from COMSOL Multiphysics, a finite element environment. Then, uncertainties are considered within soil characteristics. The random response is analysed by examining the trajectories of the drill-string axis.

1 INTRODUCTION

In order to satisfy current needs for exploration and extraction of materials from high depths in relatively economical conditions, the shape of oil-wells has evolved from the most simple vertical geometries to complex curved holes. For this reason, in an attempt to capture the dynamics of drill-strings under large displacement configurations, a Cosserat Rod approach is proposed.

In this work, the borehole is considered as a vertical cylindrical geometry that confines the drill-string, being the latter subjected to contact forces in the borehole bit and lateral surface of the well, and frictional forces at the bit.

The frictional torque is introduced as proposed by Tucker and Wang (2003). The behaviour of the torque model depends on a set of parameters a_i . Results are compared with those existing on the literature, and uncertainty propagation is performed. Many distributions for a_1 are proposed in order to determine the sensitivity of the solution to a change in this parameter.

2 COSSERAT MODEL

A model capable of capturing drill-string dynamics under large displacements is sought. Along with the hypothesis of rigid cross-sections and small strains, the model is derived following the procedures described in Antman (2006) and Altenbach and Eremeyev (2013), with the following nomenclature.

Let $(\cdot)^* = (\cdot)(s_R)$ be any function of s_R ; $(\cdot)' = \frac{d(\cdot)}{ds_r}$ be a derivative in the reference parameter; $(\cdot)_0 = (\cdot) \lambda$ be a certain quantity in the reference frame; \mathbf{n} and \mathbf{m} be applied forces and moments respectively; \mathbf{f} and $\boldsymbol{\mu}$ be distributed forces and moments respectively; ρ be the actual mass density, ρ_0 the reference mass density; E be the elastic young modulus; and G be the shear modulus.

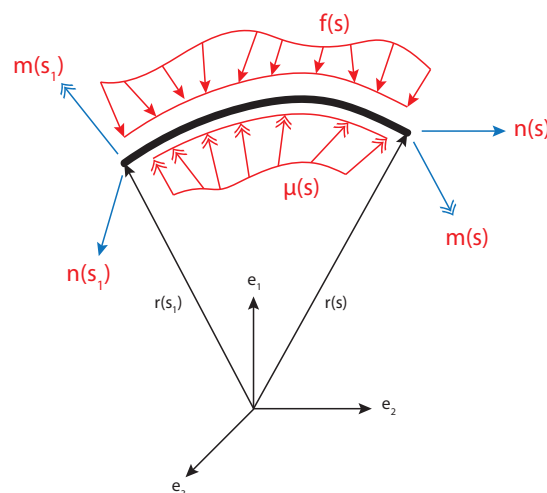


Figure 1: Equilibrium of a rod element

Eqs. (1) and (2) define the equations of motion for the problem.

$$\mathbf{n}^{*'} + \mathbf{f}_0^* = \rho_0^* A^* \frac{d^2}{dt^2} (\mathbf{r}^*) \quad (1)$$

$$\mathbf{r}^{*'} \times \mathbf{n}^* + \mathbf{m}^{*'} + \boldsymbol{\mu}_0^* = \frac{d}{dt} (\mathbf{K}_2^*) \quad (2)$$

If principal axes of inertia are considered, the vector K_2^* has the expression of Eq. (3) where $\boldsymbol{\omega}$ represents the angular velocity vector of the cross-sections.

$$\mathbf{K}_2^* = \begin{bmatrix} \rho_0^* I_{11} \omega_1^* \\ \rho_0^* I_{22} \omega_2^* \\ \rho_0^* I_{00} \omega_3^* \end{bmatrix} \quad (3)$$

Quaternion rotations are used to relate the rotation matrix with angular velocities ω_j .

2.1 Constitutive equations

Finally, the model requires a proper definition for the constitutive relations for the material in-use. For this purpose, the chosen set of equations coincides with the ones presented by (Linn et al., 2012).

Let \mathbf{u} , \mathbf{v} be vectors associated to the current configuration, where \mathbf{u} is the Darboux vector that describes orientation change for the directors of the cross-sections along the central axis of the curve, and \mathbf{v} is the tangential vector to the curve. In the same manner, let \mathbf{u}_0 , \mathbf{v}_0 be vectors associated to the reference space, with analog definitions for a reference configuration. Then, their difference can be interpreted as an angular strain and a linear or translational strain.

Thus a simple constitutive model can be written as per Eqs. (4), (5), (6) and (7).

$$\mathbf{n} = \tilde{\mathbf{K}}(\mathbf{v} - \mathbf{v}_0) \quad (4)$$

$$\mathbf{m} = \tilde{\mathbf{J}}(\mathbf{u} - \mathbf{u}_0) \quad (5)$$

$$\tilde{\mathbf{K}} = \begin{bmatrix} K_{11} & 0 & 0 \\ 0 & K_{22} & 0 \\ 0 & 0 & K_{33} \end{bmatrix} = \begin{bmatrix} GA & 0 & 0 \\ 0 & GA & 0 \\ 0 & 0 & EA \end{bmatrix} \quad (6)$$

$$\tilde{\mathbf{J}} = \begin{bmatrix} J_{11} & 0 & 0 \\ 0 & J_{22} & 0 \\ 0 & 0 & J_{33} \end{bmatrix} = \begin{bmatrix} E I_{11} & 0 & 0 \\ 0 & E I_{22} & 0 \\ 0 & 0 & G (I_{11} + I_{22}) \end{bmatrix} \quad (7)$$

3 DETERMINISTIC DRILL-STRING MODEL

The main components of the drilling rig, with regards to its dynamical behaviour, are shown in Fig. (2). The model proposed considers concentrated masses at both ends of the rod, representing the top-drive and the BHA-bit.

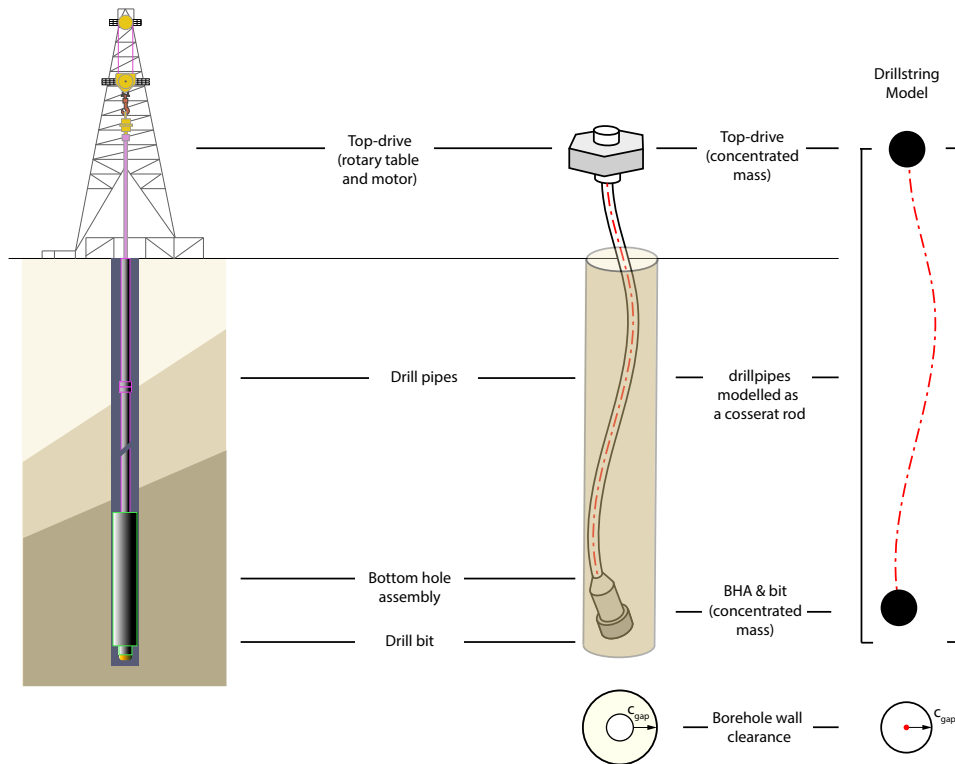


Figure 2: Drilling rig sketch and model

The drill-string is modelled using the presented Cosserat theory in [COMSOL \(2018\)](#), a commercial Multiphysics FEM software.

3.1 Drill-string basic parameters

The geometric and material properties are summarised in the following table.

Variable	Symbol	Value	Units
Mesh size	-	150	elements
Drill-string mass density	ρ_0	$8.01 \cdot 10^3$	kg m^{-3}
Drill-string length	L	$3.00 \cdot 10^3$	m
Drill-string outer radius	r_{ext}	$6.35 \cdot 10^{-2}$	m
Drill-string inner radius	r_{int}	$5.43 \cdot 10^{-2}$	m
Gravitational acceleration	g	9.81	m s^{-2}
Young's modulus	E	$2.07 \cdot 10^{11}$	N m^{-2}
Poisson modulus	ν	0.30	-
Shear modulus	G	$7.96 \cdot 10^{10}$	N m^{-2}
Top-drive effective mass	M_{top}	$5.08 \cdot 10^4$	kg
Top-drive effective rotary inertia	J_{top}	$5.00 \cdot 10^2$	kg m^2
Bit/BHA effective mass	M_{bit}	$5.00 \cdot 10^2$	kg
Bit/BHA effective rotary inertia	J_{bit}	$3.94 \cdot 10^2$	kg m^2
Borehole-wall clearance	c_{gap}	0.01	m

Table 1: Basic geometrical and material parameters for the drill-string

3.2 Rotary speed control

An optimal drilling operation implies that the drill-string angular speed ω matches exactly the target speed Ω . A control strategy is implemented in order to achieve such condition. A proportional-integral controller (PI-Controller) is considered at the top drive to maintain a constant angular velocity.

The response of the PI controller in terms of the torque at the top of the drill-string is mathematically modelled by equation 8, with $\Omega = 100$ RPM, $k_p = 200$ Nm s rad⁻¹, and $k_i = 100$ Nm rad⁻¹.

$$T_{top} = k_p(\Omega - \omega) + k_i((\Omega \cdot t - \phi)) \tag{8}$$

3.3 Contact model

A simple contact model for the borehole wall and bit is proposed. The soil is assumed to be fully elastic. For this reason, the Hooke law is adopted to represent the behaviour of the soil. A constant k_{soil} is chosen so that the drill-string remains bounded within the specified clearances.

3.4 Friction model

The proposed friction model was obtained from drilling measurements under stable drilling conditions by Tucker and Wang (2003), for constant drill-bit angular speed ($\Omega \approx 100$ rpm). It correlates the frictional torque-on-bit (*TOB*), weight-on-bit (*WOB*), depth-of-cut (*DOC*). As stated by the authors, in order to model Coulomb frictional effects it is necessary to regularise the frictional torque and rate-of-penetration so that they vanish as the drill-bit angular velocity tends to zero. Therefore, the following expression is considered, with $\epsilon = 2$ rad s⁻¹ and a varying angular speed ω .

$$TOB = (-a_1 + a_2 F_{bit})a_4 \frac{\omega_L^3}{(\omega_L^2 + \epsilon^2)^2} + a_3 a_4 \frac{\omega_L^3}{(\omega_L^2 + \epsilon^2)^{3/2}} + a_5 \frac{\omega_L}{(\omega_L^2 + \epsilon^2)^{1/2}} \tag{9}$$

Variable	Symbol	Value	Units
Weight on bit	WOB	100	kN
Model parameter 1	a_1	$3.429 \cdot 10^{-3}$	$m s^{-1}$
Model parameter 1	a_2	$5.672 \cdot 10^{-8}$	$m N^{-1} s^{-1}$
Model parameter 2	a_3	$1.374 \cdot 10^{-4}$	$m rad^{-1}$
Model parameter 4	a_4	$9.537 \cdot 10^6$	$N rad$
Model parameter 5	a_5	$1.475 \cdot 10^3$	$N m$

Table 2: Parameters for the Tucker and Wang friction model

4 PARAMETRIC SWEEP

With the aim of observing whether the solution experiences any significant change in its behaviour as parameters for the frictional model are varied, a parametric sweep is carried out.

Following the approach presented in (Ballaben and Goicoechea, 2018), a parametric sweep will be considered as a previous step for the stochastic analysis. The method avoids the necessity to perform a Monte-Carlo simulation for each proposed PDF.

Fig. (3) shows the behaviour of the friction model presented by Tucker and Wang (2003) for different values of the parameter a_1 . The value range adopted exhibits a maximum Stribeck effect for $a_1 = 0$ m/s, while there is a change in behaviour when its value get closer to $a_1 = 7.329 \cdot 10^{-3}$ m/s, as the effect vanishes.

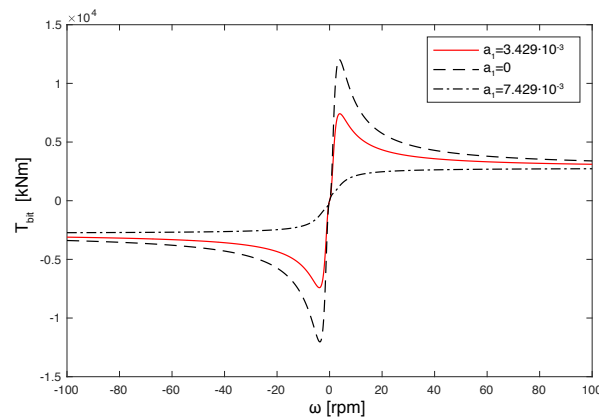


Figure 3: Variations in the frictional torque proposed by Tucker and Wang (2003) as a function of angular speed ω , in relation to changes in parameter a_1

5 STOCHASTIC ANALYSIS

Given that no information was available in relation to the data used to construct the friction model by Tucker and Wang (2003), different distributions may be considered for the parameter being studied. Also different values of the variance will be proposed to analyse the sensitivity of the response.

One possible criteria for the choice of the PDF is the Principle of Maximum Entropy. The Shannon entropy can be related to the amount of information in a random process. It is mathematically expressed as in Eq. (10). The principle states that, subject to known constraints, the current state of knowledge is best represented by the PDF that has the largest entropy.

$$S(f_X) = - \int f_X \log(f(x)) dx \quad (10)$$

Based on the procedure explained by Pérez (2007), given a certain set of constraints the following table shows the distribution that matches this principle.

Distribution	Maximum Entropy Constraint	Support
Uniform	Support within predefined interval $[a,b]$	$[a, b]$
Gamma	Positivity, $E(X) = \mu$ and $E(\ln(X))$	$[0, \infty)$
Lognormal	Positivity, $E(X) = \mu$ and $E(X^2) = \sigma^2$ value	$[0, \infty)$

Table 3: Maximum entropy probability distributions

5.1 Results

Different distributions were considered for the input a_1 parameter, and their responses are herein statistically analysed. Figure 4, depicts some of the possible outcomes for the response in time of the angular speed ω_z .

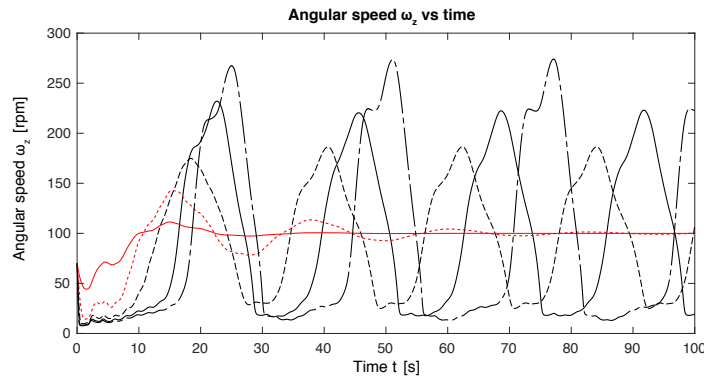


Figure 4: Different time solutions for the angular speed ω_z as parameter a_1 is varied

As expected from the variation observed in Fig. (3), there are some solutions where there is no stick-slip effect due to the vanishing of the Stribeck effect (red lines).

Fig. (5) shows the generated PDFs for the angular speed, propagated from different distributions for parameter a_1 with $E(X) = 3.4290 \cdot 10^{-3}$ m/s and $E(X^2) = 7.9474e - 07$ m²/s². The entire time history for $t = 1 : 0.1 : 100$ s is used.

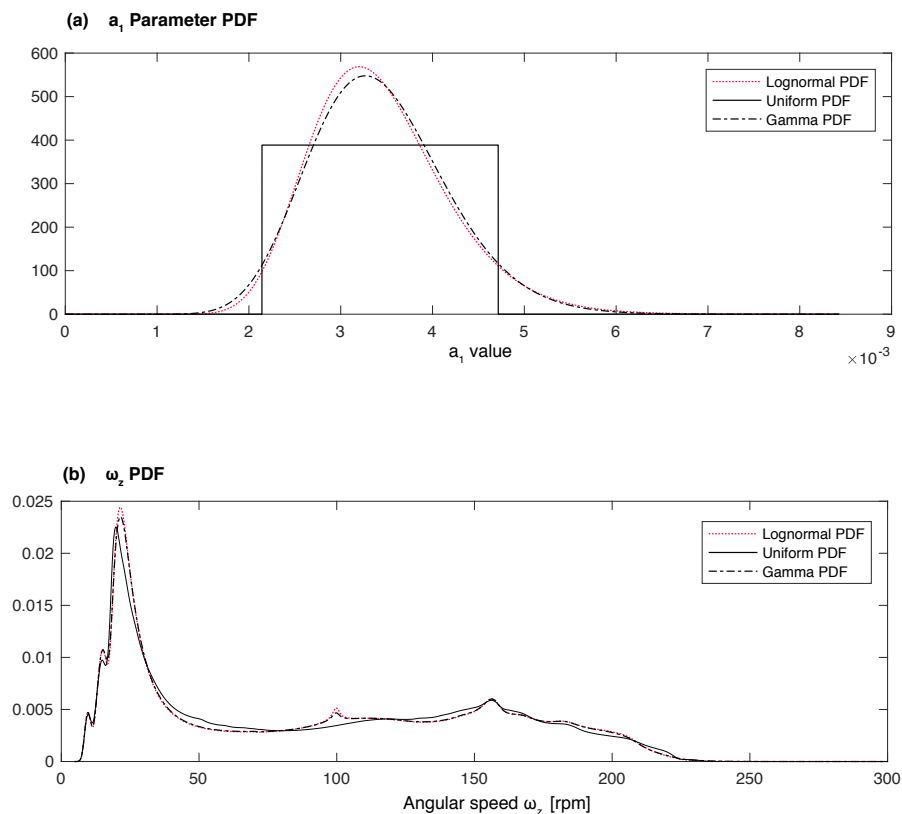
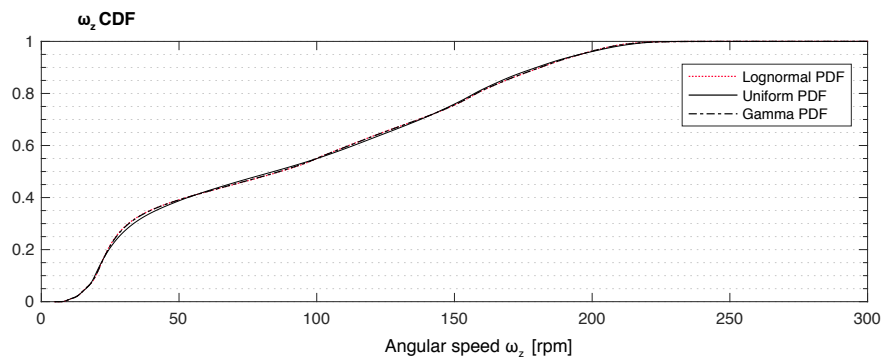
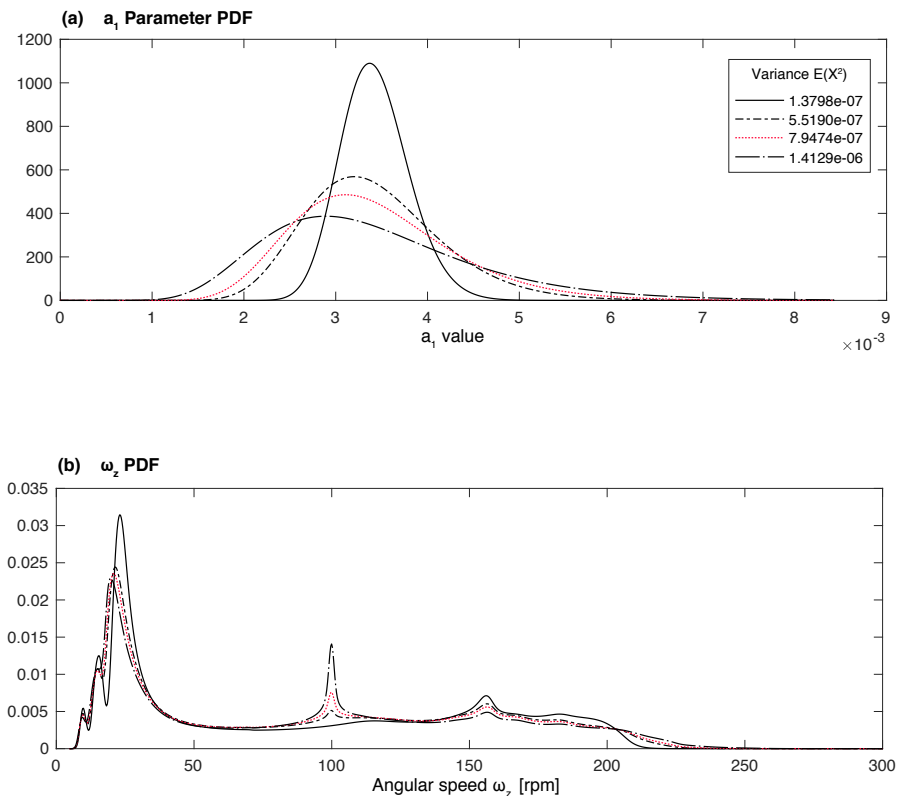


Figure 5: (a) Input a_1 PDF, $E(X) = 3.4290 \cdot 10^{-3}$ m/s and $E(X^2) = 7.9474e^{-7}$ m²/s² ;(b) output PDF for the angular speed ω

Figure 6: CDF for the angular speed ω .

A mode is observed at a low rpm value $\omega_z \leq 50$ rpm. This is linked to a stick-slip phenomenon occurring at the bit due to friction with the bore-hole. Also, all PDFs look similar in shape and magnitude, which means that the solution is not sensitive with regards to the distribution type.

Fig. (8) is constructed to evaluate the influence of the variance for a Lognormal distribution with $E(X) = 3.4290 \cdot 10^{-3}$ m/s and different values of variance $E(X^2)$.

Figure 7: (a) Input a_1 PDF, $E(X) = 3.4290 \cdot 10^{-3}$ m/s and different values of $E(X^2)$; (b) output PDF for the angular speed ω

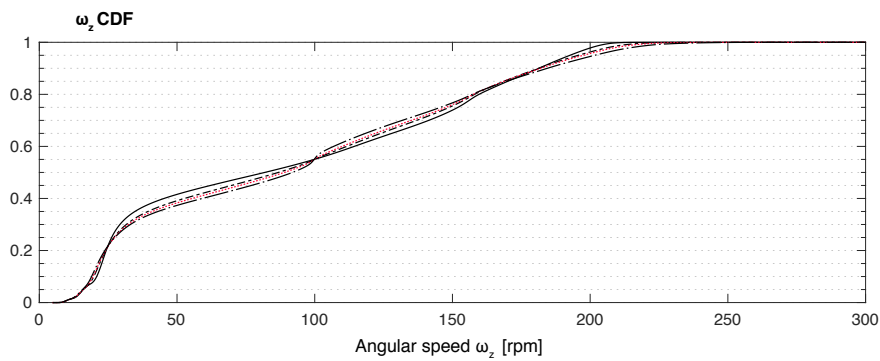


Figure 8: CDF for the angular speed ω .

For this case, again the variance of a_1 does not seem too important as there are no major changes seen in the output PDF. Note that as the variance grows, there are more chances of getting high values of the input parameter a_1 , which leads to a disappearance of the Stribeck effect where the stick-slip phenomenon is non-existent, thus the mode at $\omega_z \approx 100$ becomes more prominent.

Fig. (10) depicts the behaviour of the stick phase with regards to a variation of parameter a_1 . In this case, the shape of the distribution is affected by a change in the variance of the input parameter.

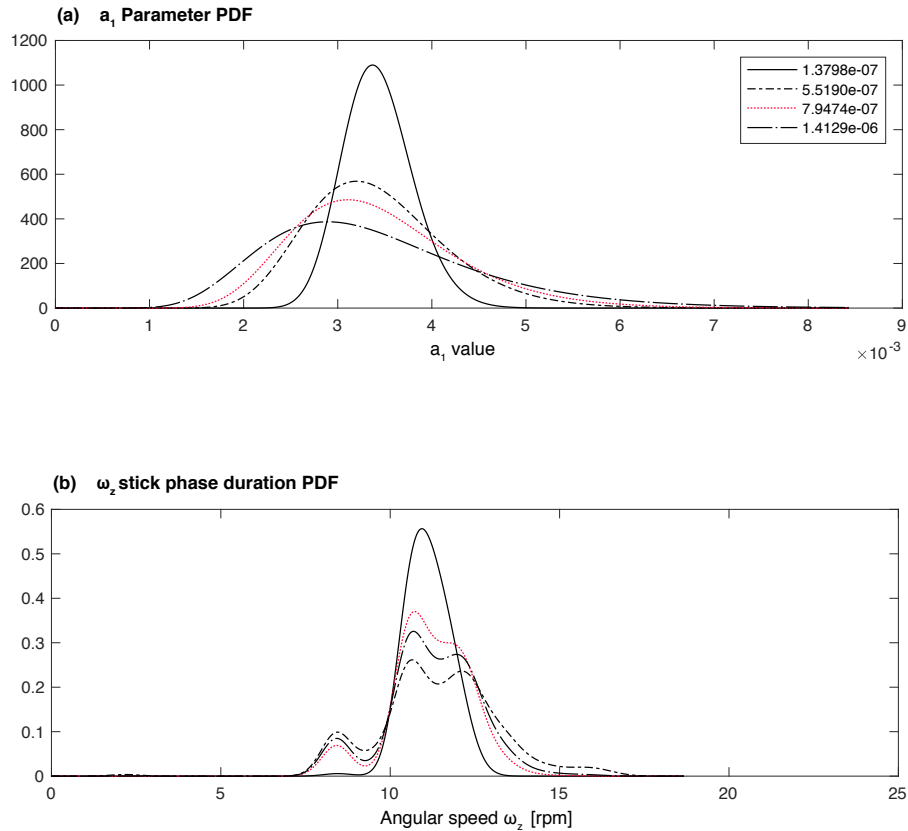


Figure 9: (a) Input a_1 PDF, $E(X) = 3.4290 \cdot 10^{-3}$ and different values of $E(X^2)$; (b) output PDF for duration of the stick phase of the angular speed.

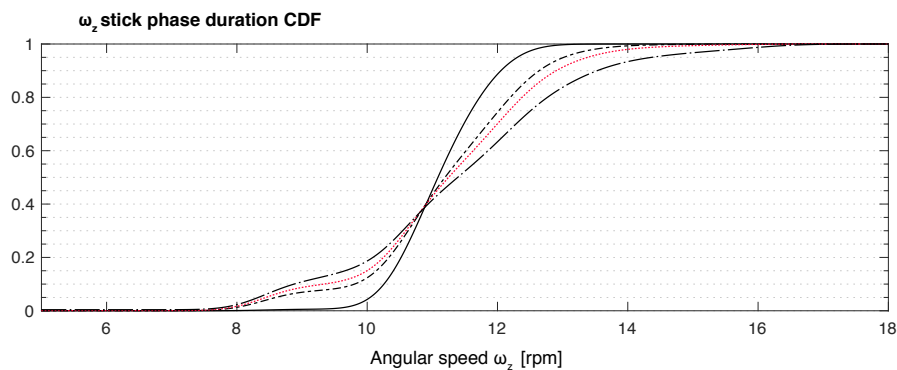


Figure 10: CDF for duration of the stick phase of the angular speed.

6 CONCLUSIONS

In this work, a drill-string was successfully modelled by means of a Cosserat Rod theory under the COMSOL (2018) environment. A stochastic distribution for the a_1 parameter from the friction model was proposed and the results were analysed.

On the one hand, the PDF for the angular speed, as generated in this work, is not sensitive to the input a_1 distribution type. It is only affected by a variation of the mean and variance values. On the other hand, the duration of the stick phase shows dependency on the parameter a_1 .

Stable operations would imply, at least, the existence of one mode at the target speed $\Omega = 100$ rpm. Therefore, as shown in Fig. (8), stable operation is not likely to occur for the lower values of $E(X^2)$.

REFERENCES

- Altenbach H. and Eremeyev V.A. *Generalized Continua from the Theory to Engineering Applications*, volume 541. Springer Science & Business Media, 2013. ISBN 978-3-7091-1370-7. doi:10.1007/978-3-7091-1371-4.
- Antman S.S. *Nonlinear Problems of Elasticity*, volume 115. Springer Science & Business Media, 2006. ISBN 978-1-4419-7054-1. doi:10.1007/978-1-4419-7055-8.
- Ballaben J. and Goicoechea H.E. An alternative to Monte Carlo simulation method. In *MECOM*. 2018.
- COMSOL. COMSOL Multiphysics®. 2018.
- Linn J., Lang H., and Tuganov A. Geometrically exact Cosserat rods with Kelvin – Voigt type viscous damping. *The 2nd Joint International Conference on Multibody System Dynamics*, 2012.
- Pérez A. *Problemas de máxima entropía y cálculo variacional*. Ph.D. thesis, Universidad Central de Venezuela, 2007.
- Tucker R.W. and Wang C. Torsional Vibration Control and Cosserat Dynamics of a Drill-Rig Assembly. *Meccanica*, 38(1):143–159, 2003. ISSN 0025-6455.